Advanced lab course for Bachelor's students

Versuch T1

Particle detectors and radiation protection

November 2021

Prerequisites

- Passage of charged particles through matter
- Interactions of photons and matter
- Gasdetectors
- Semiconductor detectors
- Scintillation counters
- Radiation protection

Aims of this experiment

- Operation of gas detectors, scintillation counters and semiconductor detectors
- Measurements of the absorption of radiation
- Use of measurement devices for radiation protection

Contents

References

[1] Gerd Otter, Raimund Honecker: Atome – Moleküle – Kerne,
Band I: Atomphysik, Band II: Molekül- und Kernphysik, Bo 184

[2] William R. Leo: Techniques for Nuclear and Particle Physics Experiments, Dr 155

[3] Konrad Kleinknecht: Detektoren für Teilchenstrahlung, Dr 143

[4] Walter Blum, Luigi Rolandi: Particle Detection with Drift Chambers, Dr 181

[5] Claus Grupen: Particle Detectors, Dr 189

[6] Hanno Krieger: Strahlenphysik, Dosimetrie und Strahlenschutz, Du 130

[7] Siegmund Brandt: Datenanalyse, mit Beispiel- und Übungsbuch, Cu 202

[8] Strahlenschutzverordnung, `http://www.bfs.de`

[9] Feuerwehr-Dienstvorschrift FwDV 500: Einheiten im ABC-Einsatz, `http://www.idf.nrw.de/projekte/pg_fwdv/pdf/fwdv500_jan2012.pdf`

[10] National Institute of Standards and Technology, `http://physics.nist.gov/PhysRefData/Star/Text/ASTAR.html`

[11] Stopping and Range of Ions in Matter, `http://www.srim.org/SRIM/SRIMPICS/STOPPLOTS.htm`

1 Semiconductor detectors

1.1 Semiconductors

Semiconductors are elements that have conductivity which is greater than that of insulators but smaller than that of conductors. By adding impurities (doping) into semiconductors, it is possible to increase their conductivity. The additional atoms used for doping are called dopants. Depending on semiconductor and dopant material, two kinds of conduction may be achieved:

- Electron conduction (n-type): By adding dopants with more free electrons per atom than the semiconductor, additional electrons are made available for charge transport.

- Hole conduction (p-type): In the reverse case, there are unoccupied electron states in the material. These unoccupied states behave as charge carriers with positive charge and thus allow charge transport.

Silicon and germanium, which are typical tetravalent semiconductors, are commonly treated with a doping concentration of $1 : 10^6$, i.e. for every 10^6 semiconductor atoms, one dopant atom is added. If n-type conduction is desired, pentavalent atoms such as phosphorous or arsenic are used. To achieve p-type conduction, trivalent elements such as boron or indium are added.

In the band model, doping adds additional electron energy levels between the valence and conduction bands. In n-doped materials, so called donor levels are added close to the conduction band, their distance in energy is $\mathcal{O}(kT)$ from the conduction band. The additional energy levels lead to a heightened Fermi level (see fig. 1). Thus, thermal activation is facilitated and the concentration of negative charge carriers is increased far beyond the intrinsic value. Analogously, for p-doped materials, the concentration of positive charge carriers is increased by the addition of acceptor levels close to the valence band.

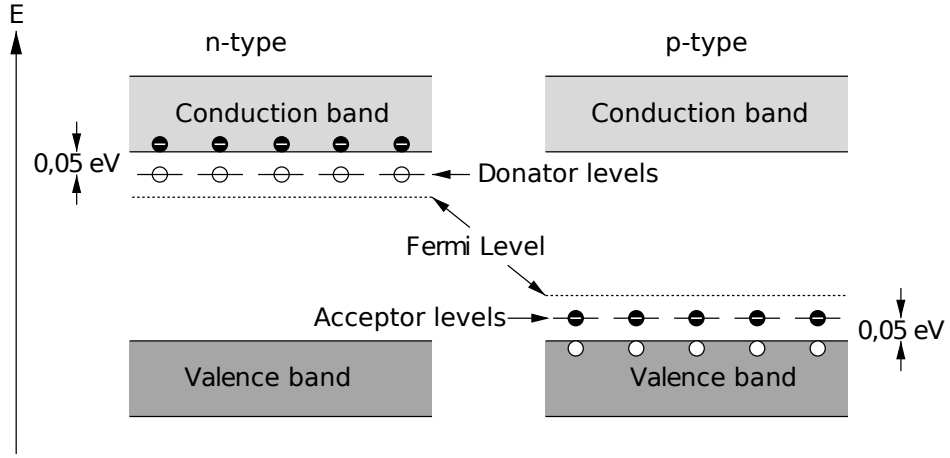

Figure 1: Band structure of p- and n-doped semiconductors.

1.2 pn-junctions

If n- and p-doped semiconductors are connected, a so called pn-junction is formed (see fig. 2). In thermal equilibrium, the Fermi levels of both materials align, thus shifting the individuals bands accordingly. The main charge carriers of both materials cross the border to balance the charge carrier concentration. The border region between the materials is thus free of charge carriers. This so called "depletion region" of distance d covers a voltage V_C. In the depletion region, electrons and holes recombine.

If a bias voltage is applied to the pn-junction (see fig. 3), the depletion region is enlarged. In principle, it is then very similar to an ionisation chamber. If an ionising particle traverses the depletion region, elastic scattering with semiconductor atoms created electron-hole pairs. The applied electric field moves these charge carriers to the cathode and anode, respectively, thus creating a measurable electric pulse.

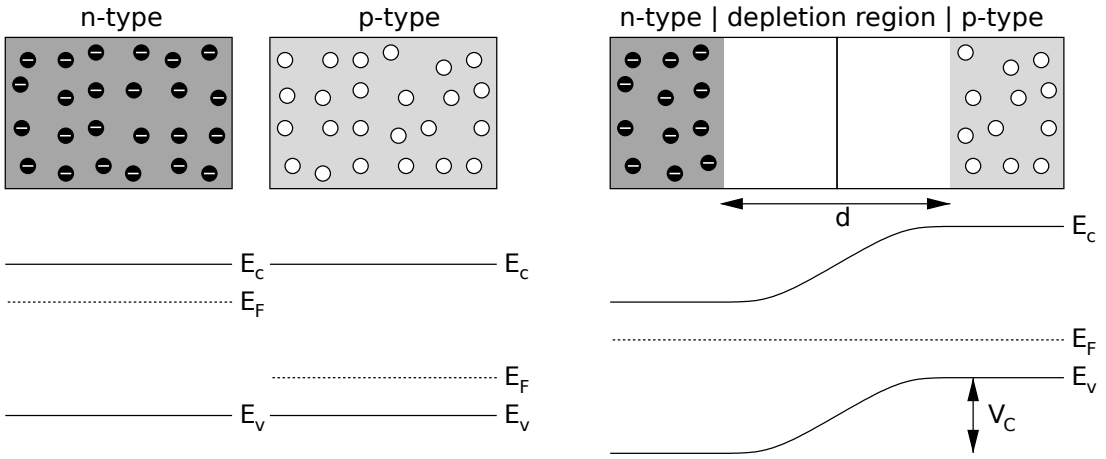

Figure 2: left: p- and n-doped semiconductors shown sepatarely, right: pn-junction.

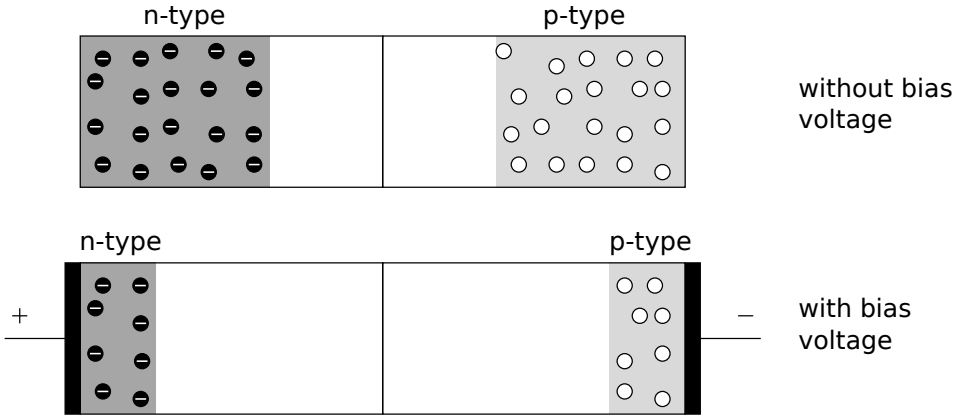

Figure 3: pn-junction with bias voltage applied.

1.3 Ionisation in the depletion region

If an ionising particle enters the depletion region, energy is transferred to the valence electrons, which are thus lifted into the conduction band and leave behind holes. The electrons relax by exciting either additional electron-hole pairs or lattice oscillations (phonons). The ionisation stops when the energy of the excited electrons is not any more sufficient to excite additional electron-hole pairs. In the band model, the electrons are now located near the lower edge of the conduction band. Holes in lower energetic levels are replaced by higher energetic ones (electrons "fall down" from the higher energetic states).

The average amount of energy w needed for the creation of an electron-hole pair in a doped semiconductor is about an order of magnitude less than for gases and about a factor of 30 less than for scintillators. Typical values for gases (e.g. in ionisation chambers) are 30 eV, for scintillators even 100 eV. Experimentally determined values for semiconductors are $w = 3{,}6\,\text{eV}$ for silicon and $w = 2{,}8\,\text{eV}$ for germanium. These values are larger than the bandgaps E_g of the respective materials (Silicon:$E_g = 1{,}1\,\text{eV}$, germanium: $E_g = 0{,}8\,\text{eV}$) because part of the absorbed energy is transmitted into phonons. Independent of the kind and total energy of traversing particle, the absorption of an energy E leads to the creation of E/w electron-hole pairs.

1.4 Properties of semiconductor detectors

1. **Proportionality:** If a particle deposits all its energy in the sensitive volume, the measured pulses are proportional to the energy. In addition to their detection, this allows for an energy measurement of the particle (spectroscopy). Since only thin detector layers are necessary to absorb α- or

β-particles, semiconductor detectors are well suited for the spectroscopy of these particles. For high-energetic particles, which traverse the sensitive volume without depositing all of their energy, spectroscopy is not possible, since the electric signal is only proportional to the deposited energy.

2. **Energy resolution:** Since each incoming particle creates a number of free charge carriers that is much larger than in e.g. an ionisation chamber, the measured pulses are much less sensitive to statistical fluctuations. Thus, the width of the pulse height spectrum is much smaller and energy measurements are more accurate. Resolutions of up to $\Delta E/E < 1\,\%$ are achievable. An example of a measured energy spectrum of ^{60}Co is shown in fig. 4. For comparison, the spectrum was recorded twice, once with a Ge(Li) semiconductor detector and once with a NaI(Tl) scintillation counter.

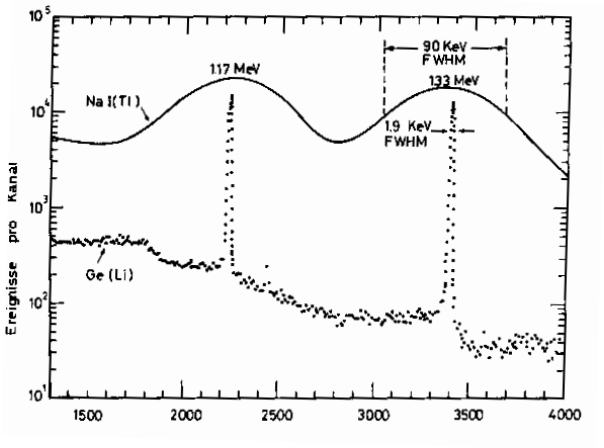

Figure 4: Energy spectrum of ^{60}Co, measured with Ge(Li) semiconductor detector and a NaI(Tl) scintillation counter, respectively.

Using the relationship $\Delta E/E \propto 1/\sqrt{n} = \sqrt{w/E}$, where n is the charge carrier density, the energy resolution of a semiconductor detector relative to that of a scintillation counter can be approximated as

$$\frac{(\Delta E/E)_{\text{semi.}}}{(\Delta E/E)_{\text{scint.}}} = \sqrt{\frac{w_{\text{HL}}}{w_{\text{Sz}}}} \approx \sqrt{\frac{3\,\text{eV}}{100\,\text{eV}}} = 0{,}2$$

In contrast to e.g. proportional counter tubes, semiconductor detectors do not have any intrinsic signal amplification. Therefore, they are sensitive to noise caused by random band transitions of electrons ("dark current"). This behavior is thermally activated and therefore governed by the Boltzmann factor $\exp(-E_g/k_BT)$. To achieve a sufficient energy resolution, it may be necessary to cool the detector.

3. **Time resolution:** Free charge carriers are created on a timescale of 1 ps. The time resolution is therefore mostly limited by the subsequent electronics, such as the amplifier. Using well tuned charge sensitive amplifiers, signal rise times of about 1 ns are achievable.

1.5 Practical uses of semiconductor detectors

1. **α-particles:** Because α-particles are emitted in a relatively small energy range of 4 to 10 MeV, the good energy resolution of semiconductor detectors is very useful for α-spectroscopy. When using silicon, depletion regions with a thickness of 100 μm are sufficient.

2. **β-particles:** β-particles have a larger range than α-particles, which increases the needed thickness of the depletion region. Although β-spectra are distorted by (back-)scattering effects in the lower energy regions, the cutoff energy may be determined (Kurie plot, after Franz Kurie).

3. **γ-radiation:** Using germanium, it is possible to create very large sensitive volumes, which even allow for the detection of γ-radiation. However, the very small band gap E_g value leads to a large

dark current. To reduce noise, it is thus necessary to cool the detector, e.g. using liquid nitrogen. This way, a very good resolution may be achieved for γ-spectroscopy (see fig. 4).

4. **Neutron detection:** Uncharged particles such as neutrons cannot be directly detected using semiconductor detectors. However, neutrons participate in interactions with the atoms' nuclei. In these interactions, charged particles are created, which can then be detected. This allows for neutron spectroscopy. When a thin layer of e.g. ^{6}LiF is applied to the surface of the detector, incoming neutrons may create α-particles, which are detectable. However, the sensitivity of such detection schemes is relatively low.

5. **Track reconstruction:** Using lithography, it is possible to create very small structures on semiconductors. They may thus be separated into many small segments, which allows for a precise spatial measurement. By placing multiple such detector layers in sequence, an accurate track measurement is possible.

1.6 Surface depletion detectors

In this experiment, a so called **surface depletion detector** is used. Such detectors are manufactured by applying a thin metal layer (mostly gold), which then acts like a pn-junction. This manufacturing process is simpler than that of a proper pn-junction detector. Because of the low penetration depth of α-particles, surface depletion detectors are well very suited for their detection.

2 Scintillation counters

2.1 Working principle of scintillation counters

Scintillation counters are among the most commonly used devices for detection of radiation. A schematic of such a counter is shown in fig. 5.

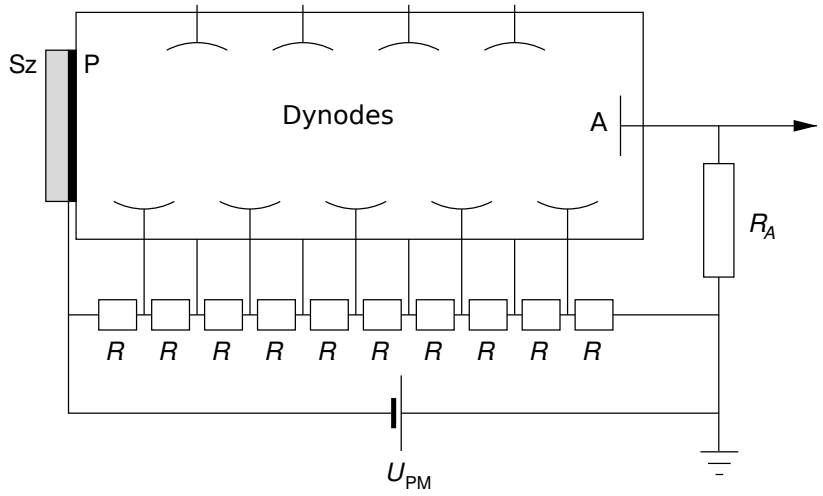

Figure 5: Schematic of a scintillation counter

Particles emitted from the source onto the scintillator material Sz cause light flashes in the material. The flashes cause emission of electrons at the photo cathode P. Using a system of dynodes, which initiate emission avalanches, the number of photo-electrons is increased by a factor between 10^6 and 10^8. When the electrons reach the anode A, they cause a measurable voltage pulse at the resistor R_A. The pulse is standardised by a pre-amplifier and discriminator and may then be registered.

2.2 Scintillator materials

When particles traverse matter, atoms are excited. Scintillator materials are luminescent, i.e. the excited atoms relax by releasing energy in form of light. This may happen in one of two different ways:

- Excited electrons instantly ($t < 10\,\text{ns}$) fall back to lower energy levels. This is called fluorescence.
- The atom enters a metastable state with a lifetime between some micro-seconds and multiple hours, depending on the material. This is called phosphorescence.

The emission of light in one of these processes is called scintillation. However, this phenomenon can only be used to detect radiation if the relaxation time is rather small ($t < 1\,\mu\text{s}$).

For experimental purposes it is desired that the scintillator material transforms as much of the traversing particle's energy as possible into light. The material should also be transparent for the emitted light and light pulses should be short. Some commonly used materials fulfilling these criteria:

- Doped anorganic crystals like NaI(Tl) or LiI(Eu).
- Organic materials, mainly aromatic hydrocarbons, in plastic or liquid supporting materials or in crystalline form.

In the lab course, NaI(Tl) and plastic scintillators are used. They may be operated with a photo-multiplier (see chapter 2.3).
The band structure description of the fluorescence process of anorganic scintillator materials is shown in fig. 6. When absorbing the energy amount E_1, electrons are lifted from the valence into the conduction band. There, they are mobile. If they immediately fell back to their previous state, the emitted photon's energy would exactly correspond to that of the initial photon. At this energy, the photon could be absorbed again, and the scintillator material would thus be opaque for the emitted photon. In order to avoid this, activator atoms such as thallium are used. They introduce additional energy levels between valence and conduction band. By exciting lattice vibrations, electrons in the conduction band can transition into these states without emitting a photon. When they subsequently fall from the activator states to the valence band, they emit a photon of energy E_2, to which the scintillator is transparent. The probability of exciting an electron straight from the valence band into one of the activator states is negligible because of the small number of activator atoms. Because of the high mobility of electrons in the conduction band, transitions from there into the activator states are much more likely.

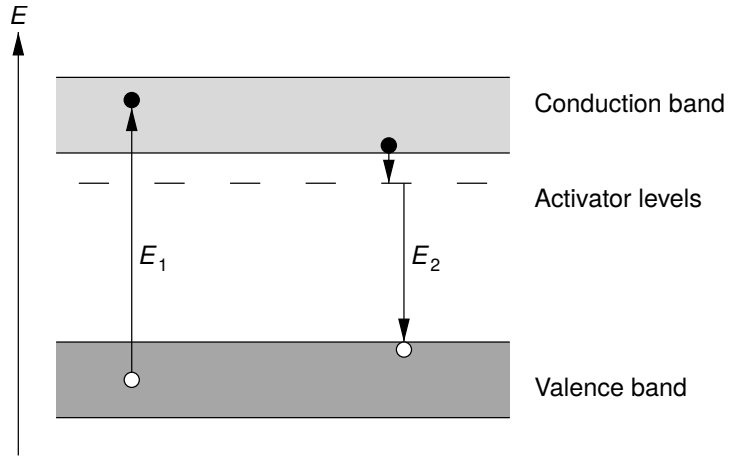

Figure 6: Band model interpretation of the fluorescence process of an anorganic scintillator.

A schematic of the fluorescence process of organic scintillator materials is shown in fig. 7. Organic scintillators commonly consists of two components, namely the fluorescing material and a mechanically supporting material. When a particle traverses the material, an electron is lifted from the ground level A into the excited state B (This transition obeys the Franck-Condon principle, see e.g. [1]). Without emitting any radiation, the electron passes into the metastable state C. The energy difference is released as heat. The further transition into state D causes the emission of the scintillation light, to which the scintillator material is transparent. Through further radiation-less transitions, the electron once more reaches state A.

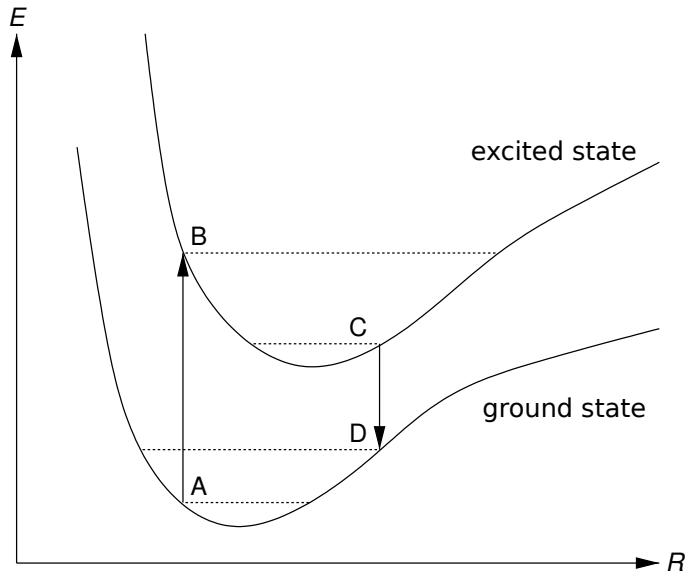

Figure 7: Fluorescence process of an organic scintillator materials. R is the spatial distance between atoms in the molecule.

2.3 Photomultipliers

Photomultipliers are used to convert the scintillation light into measurable electric pulses. They consist of a vacuum tube, on the face side of which there is a photocathode. Incoming light flashes release electrons from this cathode, which are focussed onto a system of 10 to 16 dynodes. The dynodes form a "potential staircase" with a step height of 50 to 100 V. Each of the dynodes is capped with a special coating that facilitates emission of secondary electrons. When an electron hits the first dynode, multiple electrons are released from it. Because of the potential difference between the dynodes, the electrons are accelerated towards the next dynode and the process repeats. The result is an avalanching process, which amplifies the initial signal by a factor between 10^6 and 10^8 and leads to a measurable voltage pulse.

A disadvantage of photomultipliers is the frequent emission of random pulses (noise), which is caused by the emission of single electrons at the photocathode or the dynodes. Because they follow the Fermi"=Dirac distribution, electrons constantly leave the metal surfaces even at room temperature. Furthermore, photomultipliers are sensitive to magnetic fields, which deflect electrons from their paths. To avoid this, the photomultiplier tube may be surrounded by a ferromagnetic material to screen any magnetic fields.

Often times, it is not possible to place the scintillator material in direct optical contact with the photocathode of the photomultiplier. Commonly, this happens when the cross-section of the scintillator is larger than the photocathode or when the scintillator is to be used in a large magnetic field. In these cases, a so called light guide is placed between scintillator and cathode. Light guides use total reflexion to transfer the light to the cathode without causing any losses. Light guides commonly consist of acrylic glass, which is easy to form in arbitrary ways.

Using a combination of scintillator and photomultiplier, it is possible to record energy spectra. However, the sensitivity, i.e. the probability of an incoming photon to excite a cathode electron, of the photocathode is in general wavelength dependent. Thus, to obtain energy spectra, the cathode material has to be chosen with the desired energy window in mind (see fig. 8).

2.4 Pulse height spectrum

If one uses a Multi-Channel Analyser (MCA) to record the energy spectrum of γ-radiation with an energy of 2 MeV, a result as shown in fig. 9 is obtained. This spectrum is the result of different interaction processes between γ-radiation and scintillator material.

- **Photo spectrum**: An electron is released from an inner shell via the photo effect. The energy of such an electron is $E_\mathrm{e} = E_\gamma - E_B$, where the second term represents binding energy. For NaI(Tl),

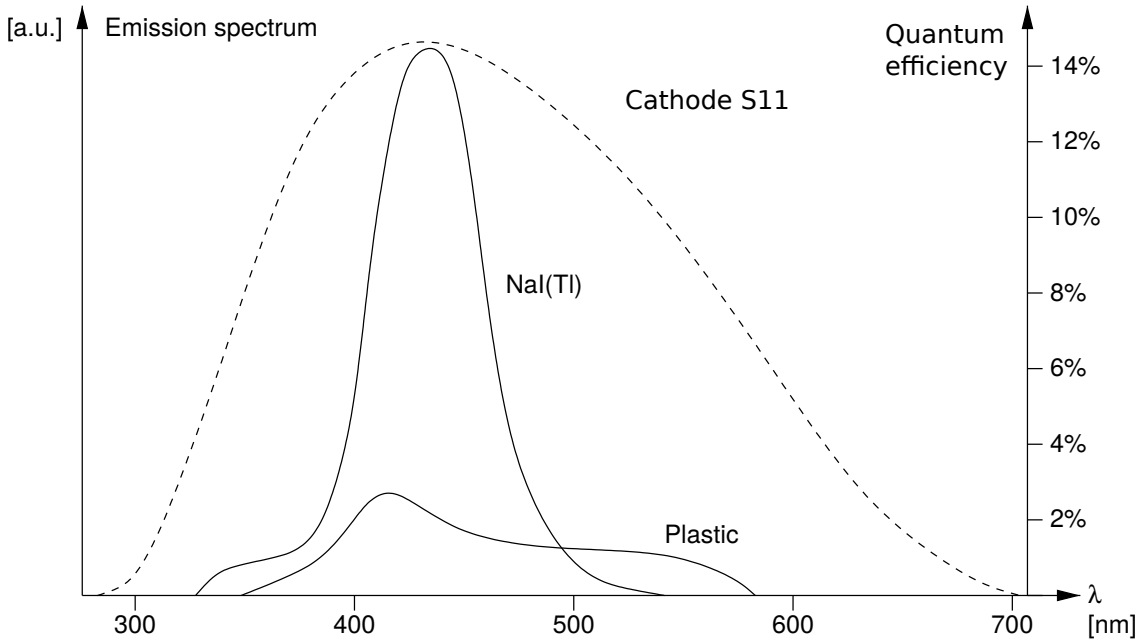

Figure 8: Emission spectra of scintillator materials (solid lines) and sensitivity distribution of a photocathode (dashed line).

where an electron is removed from the K shell of an iodine atom, the binding energy is $E_B = 36\,\mathrm{keV}$. The unoccupied state left behind by the electron is filled by an electron from one of the higher shells, which leads to the emission of x-ray photons, which may again be absorbed via the photo effect. Absorption of these secondary photons in the scintillator causes an additional peak with energy E_γ. X-ray photons that leave the scintillator material cause a peak with energy $E_\mathrm{e} = E_\gamma - E_B$. Because of the limited resolution of the detector, not two sharp lines, but rather a Gaussian distribution is observed. The energy dependence of the cross-section of the photo effect may be quantified as follows:

For energies that are not too large relative to the rest energy $m_\mathrm{e}c^2$ of the electron:

$$\sigma_\mathrm{Photo} \propto Z^5 E_\gamma^{-7/2}$$

For $E_\gamma \gg m_\mathrm{e}c^2$:

$$\sigma_\mathrm{Photo} \propto Z^5 E_\gamma^{-1}$$

Where Z is the charge of the scintillator nuclei in units of the elementary charge and E_γ is the energy of the absorbed photon.

- **Compton spectrum**: Inelastic scattering of photons and quasi free electrons is called Compton scattering. The energy of an electron that is released from the material in this way does not only depend on the energy of the incoming photon, is also a function of the scattering angle. The energy is maximal for central collisions, where the photon is back-scattered. The maximal energy E_C is called Compton edge. The continuous Compton spectrum arises when the back-scattered photon leaves the scintillator material undetected. Otherwise, the photon contributes to the photo peak. An additional peak at E_R is the result of photons that are scattered back into the sensitive region via interaction with the surrounding material. The energy dependence of the cross-section of the Compton effect may be quantified as follows:

$$\sigma_\mathrm{Compton} \propto Z \frac{\ln E_\gamma}{E_\gamma}$$

- **Pair production spectrum**: If the energy of an incoming photon is larger than twice the rest energy of the electron, the photon may transition into an electron-positron pair. Because energy

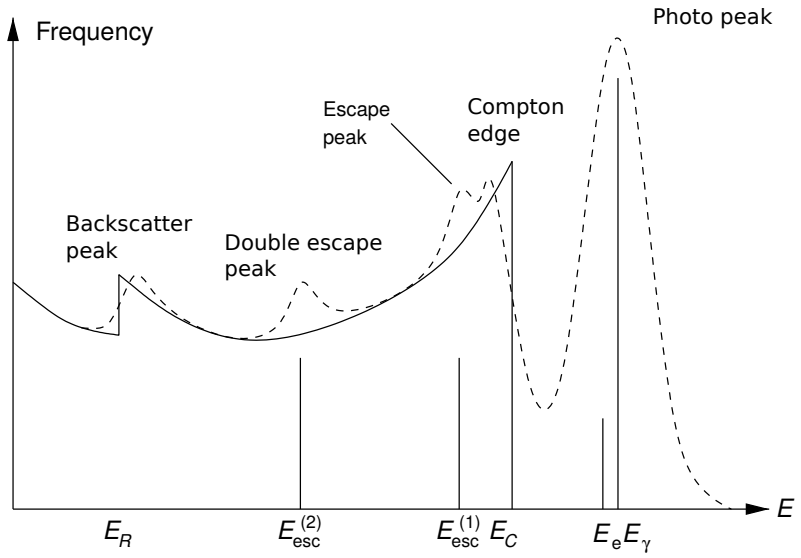

Figure 9: Schematic of the theoretical (solid lines) and measured (dashed lines) spectrum of γ-radiation at an energy of about 2 MeV, as recorded using a NaI(Tl)-scintillator

and momentum must be conserved in this reaction, it is only possible in close proximity of a nucleus. Positron and electron form a bound state which is called positronium, which is unstable and dominantly decays into two photons with energy $E_\gamma = m_e c^2 = 511\,\mathrm{keV}$. Because one (or both) of these photons may leave the sensitive volume undetected, a so called "(double-)escape peak" is observed at $E_{\mathrm{esc}}^{(1)}$ ($E_{\mathrm{esc}}^{(2)}$). The total cross-section at high energies is

$$\sigma_{\mathrm{Pair}} \propto Z^2 \ln E_\gamma$$

Question: Which peaks do you expect for the source used in the lab course (^{137}Cs), if the photons emitted by this source of β^--radiation have an energy of $E_\gamma = 661{,}6\,\mathrm{keV}$?

2.5 Properties and use cases of scintillation counters

- **Time resolution:** Specialised organic scintillator materials have a very high time resolution, which allows for the measurement of high pulse rates. A time resolution of order 100 ps is possible. Such scintillation counters are used as fast triggers for other detectors or to measure time intervals.

- **γ-spectroscopy:** Anorganic scintillators such as NaI(Tl) are well suited for γ-spectroscopy. The included iodine atoms ($Z = 53$) have a high photo effect cross-section. Furthermore, in contrast to semiconductor detectors, large detection volumes are possible. Additionally, the proportionality between photon energy and emitted light is almost exact. A spectrum one might record using a NaI(Tl) scintillator is shown in fig. 8.

  A disadvantage of scintillation counters is the large amount of energy needed for electron release (25 eV) and the low detection efficiency (25 %) of photons at the cathode. So on average, an energy of about 100 eV is needed per detected photo electron.

- **Form:** Scintillation counters may be formed in a wide range of shapes and sizes. This is especially true for plastic and liquid scintillator materials.

3 Ionisation chambers

The ionisation chamber is one of the oldest concepts for the detection of radiation. Due to its simple working principle, it is still in common use today. A schematic is shown in fig. 10.

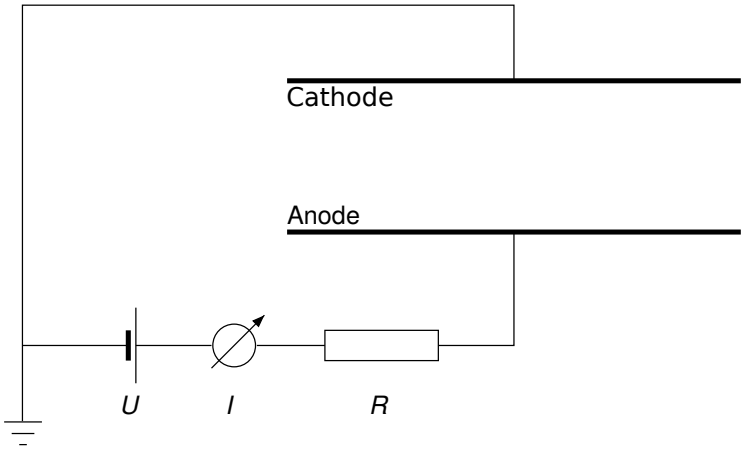

Figure 10: Schematic view of an ionisation chamber.

The amount of energy that is necessary to create an electron-ion pair is independent of the energy of the ionising particle. In gases it is about 30 eV. E.g. if the ionising particle deposits 1 MeV of energy in the chamber, about $3 \cdot 10^4$ electron-ion pairs are created, which corresponds to a separated charge of about $5 \cdot 10^{-15}$ C for each charge sign. Depending on the construction of the chamber, the charge is either integrated into a constant current (Current mode) or gives separate short voltage pulses for each charge carrier (Pulse mode).

In the lab course, ionisation chambers are used in **Current mode**. At a typical value for the capacity between the electrodes of $C = 10^{-12}$ F and using a resistance of $R = 10^{12}\,\Omega$, a time constant of 1 s is achieved. This time constant is large compared to the time needed for the ions to reach the electrodes (≈ 1 ms). Therefore, the chamber cannot resolve single particle transits, but rather measures a signal that is integrated over a longer period. This kind of ionisation chamber is used e.g. for dose and dose rate measurements in radiation protection applications and for intensity monitoring at particle accelerators. The measured charges/currents are extremely small, which makes strong electric insulation necessary. Also, the recombination of ions and electrons may distort the linear relationship between absorbed energy and detected current, which may impede effortless interpretation of results.

4 Range of radiation in matter

4.1 Range of α-particles

The Geiger-Nuttall law

Emission of α-particles is governed by an empiric relationship between the range R and decay probability λ. It was discovered in 1911 by Hans Geiger and John Mitchell Nuttall:

$$\log \lambda = C_1 + C_2 \log R, \tag{1}$$

Where C_1 and C_2 are constant. Using Geiger's law for the relationship between energy E and range R of a particle

$$R \approx \text{const} \cdot E^{1,5}, \tag{2}$$

the Geiger-Nuttal law may be written as

$$\log \lambda = C_1' + C_2' \log E. \tag{3}$$

This relationship is curious if we consider that the decay probabilities cover a range of 25 orders of magnitude while the energies only vary between 2 and 10 MeV. A theoretical description of this relationship was subsequently found in the quantum mechanical treatment of the α-decay (tunnel effect).

Energy deposition by α-particles in matter

Most of the energy deposited by α-particles and in general heavy charged particles is transmitted via inelastic scattering with shell electrons. The atom that serves as the interaction partner is excited or even ionised via the Coulomb interaction. The interaction with electrons does not significantly alter the trajectory of heavy particles, which is mostly linear. Therefore, the range of α-particles is equal to the distance between emission and end point.

Depending on their velocity, particles deposit an energy amount dE per unit length dx. The ratio $-dE/dx$ is called average energy loss per unit length[1]. It is governed by the Bethe-Bloch formula. By integrating the reciprocal quantity dx/dE over the available energy range, one obtains the average range $\overline{R}$ of the particle:

$$\overline{R} = \int_{E_0}^{0} \frac{dx}{dE}\, dE = \int_{E_0}^{0} \frac{1}{dE/dx}\, dE. \tag{4}$$

If the energy dependence $\frac{dE}{dx}(E)$ is known, a range measurement may be used to determine the initial energy E_0. Due to the statistical nature of the deceleration process, R is not exactly the same for all particles. It rather follows a Gaussian probability density distribution. The differential and integrated distributions of the range parameter are shown in fig 11. The integrated distribution gives the normalised absorption curve.

By drawing a tangent line to the integrated distribution at the point where it crosses 1/2, and finding the point where the tangent line crosses the R axis, the so called extrapolated range R_{ex} is computed. It is related to the average range by

$$R_{\text{ex}} - \overline{R} = \sigma\sqrt{\frac{\pi}{2}}. \tag{5}$$

Using this formula it is possible to calculate the distribution width σ from an empirical absorption curve.

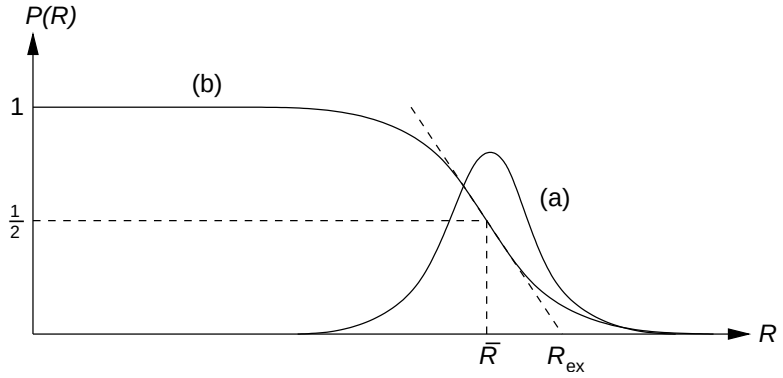

Figure 11: Differential (a) and integrated (b) distribution of the range of α-particles

The Bragg curve

The specific energy loss $-dE/dx$ is directly related to the specific ionisation, i.e. the number n of ion pairs created per unit length:

$$n = -\frac{dE}{dx}\frac{1}{w}. \tag{6}$$

Where w is the average energy needed for the creation of an ion pair. w only depends on the absorbing material (e.g. $w = 33{,}7\,\text{eV}$ for air) and not on the energy or type of ionising particle. The ionisation density n is shown in fig. 12(a) as a function of the distance covered by the particle. It is called Bragg curve. A striking feature of the curve is its large peak near the end of the trajectory. It is a result of a strong increase in the energy loss $-dE/dx$ for low particle velocities (see Bethe-Bloch formula). For a

[1]It may also be called *Bremsvermögen* or *Stopping Power* if it is interpreted as a property of the surrounding material

beam of mono-energetic particles, the range covered varies for each particle. This results in a "smearing" of the ionisation curve, which is shown in fig. 12(b).

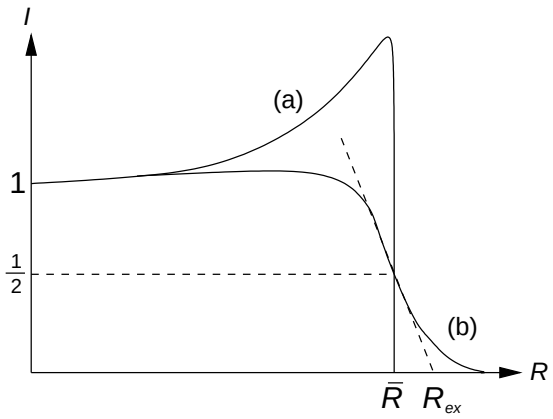

Figure 12: Ionisation curve for α-particles (Bragg curve). (a) single particle, (b) particle beam with statistical distribution of particle ranges.

4.2 Range of β-particles

In contrast to the energy deposition of heavy charged particles, which happens mainly through interaction with shell electrons, the energy loss of β-particles is mediated by three processes:

1. Scattering with shell electrons (Electron-electron scattering, so called Møller scattering): A quantitative treatment of Møller scattering leads to an expression that is similar to the Bethe-Bloch formula. It differs by an added interference term that represents the wave mechanical interaction of identical particles.

2. Elastic scattering with nuclei (Mott scattering): Described by the Rutherford scattering formula with an added factor $(1 - \beta^2 \sin^2 \frac{\theta}{2})$ that represents the electron's spin (spin-orbit coupling).

3. Bremsstrahlung: The power dE/dt radiated via Bremsstrahlung is proportional to $\ddot{x}^2$. Deceleration in the Coulomb field is described by $m\ddot{x} = -Ze^2/x^2$. Therefore, Bremsstrahlung gives large contributions only for light particles such as electrons. Following Bethe and Heitler, the energy losses due to Bremsstrahlung and ionisation are related by:

$$\frac{(dE/dx)_{\text{Brems}}}{(dE/dx)_{\text{Ion}}} = \frac{E \cdot Z}{1600\, m_e c^2} \approx \frac{E \cdot Z}{800\,\text{MeV}}. \tag{7}$$

   For an energy of $E = 800\,\text{MeV}/Z$ (about 100 MeV in air) both components are equal. Therefore, for electrons in air the energy loss due to Bremsstrahlung is negligible at energies smaller than about 10 MeV. In this energy region, the energy loss is dominated by of ionisation.

Elastic scattering with nuclei deflects electrons from their initial paths. A well collimated beam of electrons will therefore broaden as it passes through matter. Therefore, unlike heavy particles, electrons do not have a well-defined range, even if a mono-energetic beam is used. However, the maximal penetration distance R_{max} may be defined. The absorption coefficient as a function of the material thickness is monotonically decreasing and may be extrapolated to access R_{max}.

For a β-spectrum with a continuous energy distribution of the electrons, an empirical absorption law may be found:

$$\frac{I}{I_0} = e^{-\mu x}. \tag{8}$$

This simple exponential relationship is not trivial (as γ-radiation, see sec. 4.3) , but is a result of the combination of the form of the β-spectrum and multiple scattering.

The mass absorption coefficient $\mu' = \mu/\rho$ is nearly independent of Z and may be written as:

$$\mu' \left[\frac{\mathrm{cm}^2}{\mathrm{g}}\right] \equiv \frac{\mu\left[\frac{1}{\mathrm{cm}}\right]}{\rho\left[\frac{\mathrm{g}}{\mathrm{cm}^3}\right]} = \frac{17}{\big(E_{\max}[\mathrm{MeV}]\big)^{1,14}}. \tag{9}$$

This relationship allows for a rough estimation of the maximal energy $E_{\max}$ of a β-spectrum. E.g. one may experimentally find $d_{1/2}$, the material thickness that leads to an intensity attenuation by a factor of 2:

$$d'_{1/2}\left[\frac{\mathrm{g}}{\mathrm{cm}^2}\right] \equiv d_{1/2}\,[\mathrm{cm}] \cdot \rho\left[\frac{\mathrm{g}}{\mathrm{cm}^3}\right] = \frac{\ln 2}{\mu'} = 0{,}04\big(E_{\max}[\mathrm{MeV}]\big)^{1,14}. \tag{10}$$

By extrapolating the semi-logarithmic absorption curve onto a constant background (mainly Bremsstrahlung), the maximal range $R_{\max}$ may be measured. The maximal energy $E_{\max}$ and range $R_{\max}$ are empirically related by:

$$\begin{aligned} R'_{\max}\left[\frac{\mathrm{g}}{\mathrm{cm}^2}\right] \equiv R_{\max}\,[\mathrm{cm}] \cdot \rho\left[\frac{\mathrm{g}}{\mathrm{cm}^3}\right] &= 0{,}412 \cdot \big(E_{\max}[\mathrm{MeV}]\big)^{a} \\ \text{with} \quad a &= 1{,}265 - 0{,}0954 \cdot \ln\big(E_{\max}[\mathrm{MeV}]\big). \end{aligned} \tag{11}$$

The ranges of positrons and electrons may differ by up to 10 %.

4.3 Range of γ-radiation

There are multiple interactions between photons and matter:

- Photo effect
- Compton scattering
- Pair production

Consider a beam of photons incident on an absorber material and assume that each photon that participates in one of the above processes is lost from the beam. The attenuation of the beam intensity I may then be written as:

$$dI = -IN(\sigma_{\mathrm{Photo}} + \sigma_{\mathrm{Compton}} + \sigma_{\mathrm{Pair}})\,dx. \tag{12}$$

Where N is the number of absorber atoms per unit volume, x is the absorber thickness and I_0 is the initial beam intensity. By defining $\mu = N(\sigma_{\mathrm{Photo}} + \sigma_{\mathrm{Compton}} + \sigma_{\mathrm{Pair}})$ and integrating (12) one obtains the absorption law:

$$I(x) = I_0 e^{-\mu x}. \tag{13}$$

If the mass absorption coefficient $\mu' = \mu/\rho$ is used instead of the absorption coefficient $\mu\,[1/\mathrm{cm}]$, the thickness x is replaced by $d = x \cdot \rho$.

5 Radiation protection

In Germany, all work with radioactive sources and their storage is subject to so called Strahlenschutzverordnung or in short **StrSchv** (literally: "law regarding radiation protection") [8]. By default, any use of radioactive materials requires a permit issued by the government, with exceptions for sources below certain activity thresholds. To protect workers from contamination, radiation dose monitoring is required. This section is meant to give you basic knowledge about dosimetry and protection measures against ionising radiation.

5.1 Quantities / Units

In order to describe radioactive sources, a number of different measurement quantities and their associated units have been introduced. Important aspects are the strength of radioactive sources, their energy output and their effect on matter such as the human body. The most important quantities are listed here.

1. **Activity:** The activity A of a source is defined as the number of decays per unit time. It may be calculated via

$$A = -\dot{n} = n\lambda. \tag{14}$$

   where n is the number of radioactive nuclei, $\lambda = 1/\tau$ is the decay probability of a single nucleus per unit time and τ is the average lifetime of a single nucleus.

   Unit: 1 Becquerel = 1 Bq = 1 Decay/Second

   Antiquated: 1 Curie = 1 Ci = $3{,}7 \cdot 10^{10}$ Bq

   One Curie is equivalent to the activity of 1 g of radium.

2. **Ion dose:** The ion dose I is the free charge created by photons (x-ray or gamma) in air per mass unit: $I = dq/dm$.

   Unit: C/kg Antiquated: 1 Röntgen = 1 R = $2{,}58 \cdot 10^{-4}$ C/kg

3. **Energy dose:** The energy dose D is the energy deposited per mass unit by any kind of radiation: $D = dE/dm$. Unit: 1 Gray = 1 Gy = 1 J/kg Antiquated: 1 Rad = 1 Rd = 0,01 Gy

   Ion and energy dose at the same location in air are related. By using the average energy needed to create an ion pair in air $w = 33{,}7$ eV, one the energy dose D_{Air} that corresponds to an ion dose of 1 C/kg:

$$D_{\text{Air}} = \frac{dE}{dm} = \frac{dE}{dq}\frac{dq}{dm} = \frac{33.7\,\text{eV}}{1.6 \cdot 10^{-19}\,\text{C}} \cdot 1\,\frac{\text{C}}{\text{kg}} = 33.7\,\frac{\text{J}}{\text{kg}} = 33.7\,\text{Gy}. \tag{15}$$

   This calculation may be performed for human tissue analogously. Human tissue consists predominantly of water, the mass absorption coefficient of which is about 1.11 times larger than that of air. Therefore

$$D_{\text{Tissue}} = 1.11 \cdot 33.7\,\frac{\text{J}}{\text{kg}} = 37.1\,\text{Gy}. \tag{16}$$

4. **Equivalent dose:** Depending on the kind of radiation, the biological effect caused by a certain energy dose may vary. The amount of energy released by ionisation does not sufficiently quantify the danger from radiation. A quality factor Q is introduced to correct for this effect. The corrected dose is called equivalent dose: $H = Q \cdot D$.

   Unit: 1 Sievert = 1 Sv Antiquated: 1 Röntgen Equivalent Man = 1 rem = 0,01 Sv

   One sievert quantifies the energy dose of arbitrary radiation that causes the same biological effect as 1 Gy of γ-radiation. The Q factors for different kinds of radiation are thus:

Radiation	Q
γ	1
β	1
α	20
Thermal and slow neutrons	2 – 3
Fast neutrons	20

5. **Dose rate:** The dose rate $\dot{D}$ and the equivalent dose rate $\dot{H}$ is the radiation dose received per unit time.

   Unit: Gy/h or Sv/h, respectively.

5.2 The dose constant of γ-sources

The activity A of a γ-source is not sufficient to quantify the expected dose at a certain location. Depending on the source, a whole cascade of photons may be emitted per decay. To correct for this effect, the dose constant I_γ is introduced. The source is assumed to be point-like and absorption in air is neglected:

$$\dot{D} = I_\gamma \frac{A}{r^2}. \tag{17}$$

If an absorbing layer of thickness x and absorption coefficient μ is placed between source and measurement location, the dose rate is reduced as

$$\dot{D}_A = \dot{D} \cdot \exp(-\mu x). \tag{18}$$

Where $\dot{D}$ is the dose rate without any absorber material.

Using this equation, one may estimate the absorber thickness x needed to reduce the dose rate to a certain value. However, this estimation only takes into account the effect of primary photons. Secondary photons, e.g. photons that are scattered via in the absorber via the Compton effect, are neglected. The effect of secondary electrons may be incorporated by adding so-called dose build-up factor. For γ energies of more than 0,5 MeV, it may be approximated as $(1 + \mu x)$. Thus, eq. (18) is replaced by:

$$\dot{D}_A = \dot{D} \cdot (1 + \mu x) \cdot \exp(-\mu x). \tag{19}$$

5.3 Dose thresholds

There is no known lower threshold below which radioactive doses are definitely harmless for humans. The allowed dose is an interval bounded by two thresholds:

- Natural radiation dose. Either from external (cosmic radiation 0,35 mSv/year, rock 0,5 mSv/year) or internal sources (^{14}C, ^{40}K in the human body, radon in inhaled air, etc. 1,6 mSv/year).

- Doses that may be classified as obviously dangerous (e.g. if changes in the blood count or skin damage is caused).

In Germany, the Strahlenschutzverordnung defines the following dose thresholds for radioactivity from artificial sources:

1. All areas that are not specially classified:
   maximal dose of 1 mSv per year.

2. Monitoring areas (e.g. rooms used in the lab course):
   Dose rate > 1 mSv/a, which corresponds to $> 0{,}5\mu$Sv/h for 2000 working hours per year.

3. Restricted access areas (e.g. the isotope lab for experiment X):
   Dose rate > 6 mSv/a, which corresponds to $> 3\,\mu$Sv/h for 2000 working hours per year.

4. Areas that are off-limits to personnel (e.g. particle accelerators during operation):
   Dose rate > 3 mSv/h.

5.4 Contamination

An object or area is considered to be contaminated if the measured activity is at least three times larger than the naturally occurring value.

5.5 Radiation shielding

α-radiation may already be shielded by a sheet of paper. It does not penetrate the skin. Therefore, it is only dangerous if a source is ingested. This is one of the principal reasons, eating and drinking are prohibited in the lab rooms.

β-radiation may be shielded by aluminum with a thickness of a few centimeters. Aluminum is especially suited because of the low charge of its nucleus ($Z = 13$) which inhibits the production of Bremsstrahlung.

γ-radiation is best shielded my large amounts of dense matter such as lead, iron or heavy concrete (using iron or iron ore as filling material). Lead is especially suited for low γ energies, because its nuclei are strongly charged ($Z = 82$), which increases the interaction cross-section for the photo effect. Iron and concrete are used for higher γ energies, because they facilitate the construction of very thick absorption layers.

Shielding of neutrons is more complicated, especially fast neutrons tend to penetrate most materials. Commonly, a two-step procedure is used. The neutrons are first decelerated in materials with high proton content such as water or paraffin. Once they are thermalised, the neutrons are captured either in the deceleration material or in an additional capture material (e.g. boron). In both steps, secondary γ-radiation may be created, which requires additional shielding. An advantageous choice of material is heavy concrete with a large water component. It contains a large amount of protons which facilitate neutron deceleration as well as atoms with high Z that cause photon absorption.

5.6 Measurement devices

Dosimeters and dose rate monitors are used to measure the amount of radiation received while working with radioactive sources. Dose rate monitors are commonly battery powered, portable devices. They employ counting tubes or ionisation chambers to detect α-, β- or γ-radiation. For α- and γ-radiation, the displayed quantity is usually the number of pulses per second. For γ-radiation, the devices are commonly calibrated in units of the equivalent dose rate (Sv/h). For neutrons, dose rate measurements are difficult. For neutron spectra such as those prevalent in nuclear reactors, special instruments have been developed that display an approximate average value for the dose rate. In the lab course, there is a dose rate monitor that gives accurate dose rate readings (in mrem/h) for neutron energies from 10^{-2} up to 10^{7} eV. In contrast, dosimeters measure the received radiation dose and not the dose rate. Pocket dosimeters are in common use for the measurement of the daily dose. Its working principle is that of an electrometer: After being initially charged, it is slowly discharged by ionisation. The ionisation may be caused by β-radiation or free electrons created in interactions of incoming γ-radiation and the device casing. To measure monthly doses, film dosimeters are used. Judging by the discoloration of emulsion films placed behind absorbers of different strength, the dose may be estimated.

6 Performing the experiment

6.1 Measuring the absorption thickness of different detectors

6.1.1 Semiconductor detector

Mount the detector on the work bench and connect the output of the amplifier with the multi-channel analyser (MCA). (For additional information about the used NIM modules, cf. E) The MCA is connected to the computer via USB. On the PC, the measured data is processed with the Genie 2000 software. (For additional information about Genie 2000, cf. F.)

1. Install the ^{226}Ra-source in the source mount on the x-y-z translation stage. Make sure it is placed centrally with respect to the detector. Do you see all of the expected peaks?

2. Vary the distance of source and detector. At some distances, one α-peak at a time will vanish. Measure these distances as precisely as possible. Record one spectrum for the vanishing position as well as 1 mm before and after.

3. Record the spectrum for the shortest possible distance.

4. Install the collimator on the source casing. Using an appropriate stepwidth, record spectra for increasing distances between source and detector. Make sure that you cover enough distance for the ^{214}Po-α-peak to vanish completely. It may be sensible to record the spectra using a constant measurement time.

6.1.2 Ionisation chamber

The ionisation chamber consists of an electrode at ground potential and a grating to which a high voltage is applied (**Do not touch the grating!**). Also, avoid touching any of the ionisation chamber cables during the measurement. Since very small currents are measured, this may distort the result. It is a good idea to choose a sensible measurement range at the beginning to avoid changes during the experiment. Air is used as the counting gas.

1. Apply a voltage of 1 kV to the chamber and turn on the digital amperemeter. Let some time pass and adjust the amplifier so that the amperemeter shows zero current. Some fluctuation is impossible to avoid (Quantify the fluctuation by providing uncertainties!). Make sure that no α-particles reach the detector during the zeroing procedure.

2. Place the ^{226}Ra source centrally in a central position in front of the ionisation chamber. Move it as close as possible to the detector without touching the grating.

3. Starting with the smallest possible value, increase the distance between detector and source in approriate steps. Record a spectrum for each step. It may be sensible to let the setup rest for some time at each step before data-taking. This can help to reduce fluctuations (look at the multimeter!).

6.2 Measurements using the scintillation counter

Here we want to compare the energy resolution of an organic (plastic, anthracene) and an anorganic (NaI) scintillator.

6.2.1 Gamma spectrum

1. One at a time, connect the NaI(Tl) and plastic scintillators to the photo-multiplier (**Switch off the high voltage before!**). Connect the voltage supply (**Maximal voltage 1200 V!**, the usual working point is 600 V) and display the pulses on the oscilloscope.

2. For each of the scintillators, use the MCA to record a pulse height spectrum of the ^{137}Cs source. The MCA only works for positive pulses with a minimum length of about 1 μs. Therefore, it is necessary to form and amplify the pulses using the NIM modules (cf. E). Note all amplifier settings and comment on possible differences. How and why are the spectra different?

6.2.2 Absorption of γ-radiation in lead

Use the Osprey Canberra device, embedding a NaI(Tl) scintillator, to measure the absorption of γ-radiation emitted by the ^{137}Cs source in different lead absorbers. Take one spectrum for each layer and integrate the photo-peak using the Genie 2000 software. Perform a measurement without any absorber and note all necessary information about any additional absorption.

6.2.3 Absorption of β-radiation in aluminum

Connect the photo-multiplier of the anthracene scintillation counter to the high voltage supply. (**Maximal voltage 1200 V!**) Place the ^{90}Sr source in the counting chamber, use the oscilloscope to check the pulses and feed them into the counter. Use the threshold of the NIM modules to reduce background. Measure the count rate for different aluminum absorbers. Make yourself familiar with the decay characteristics of the source. Make sure to also perform measurements at distances greater than the expected range $R_{\max}$. Perform a measurement without an absorber and note down all the necessary information.

6.3 Radiation protection measurements

1. Measure the γ dose rate in 10 cm distance from the outer walls of the closed safes in the lab rooms, as well as near setups of the experiments T2 (Compton scattering), T5 (Moessbauer experiment) and T12 (Detection principles).

2. Perform contamination measurements near your experimental setup and those of experiments T2, T5, T7 and T12. Especially scrutinize the tools used to move the radioactive sources and the inside of the counting chambers. If you find any contaminations, report them to the supervisor!

7 Analysing your data

7.1 Measurement of the absorption layer thickness of different detectors

Please enclose your raw data to your report. Use appropriate formats (e.g. tables or electronic formats).

7.1.1 Semiconductor detector

1. Show one of your spectra and discuss it.

2. From the spectra, determine the distances at which α-particles **on average** cannot reach the detector anymore. Use this information to estimate the air equivalent of the thickness of the **additional** absorbing material.
   To do this, compare literature values for the range of α-particles in air (cf. [10]) with those you measured. How thick is the intrinsic unreducable absorption layer of your setup (source casing, etc.)? Estimate the uncertainty on this value.

3. Using the ^{226}Ra spectrum that was recorded at the lowest possible distance to determine a (linear) calibration curve for the MCA.
   Again, consult the literature (cf. [10]) for the α-particle range, the energy deposited in the detector and the stopping power of air. When plotting the data, consider the information you have previously gained about the absorption layer thickness and the resulting remaining range of the α-particles. Estimate the uncertainties.

4. Use the signal distance (in MCA channel numbers) of the ^{214}Po-α peaks at different distances between source and detector to again find a calibration curve of the MCA.
   Determine a relation between channel number and distance (source–detector, **total absorption layer thickness**). By scaling with the stopping power, this distance calibration of the MCA can be used to determine a (linear) energy calibration. To determine the correct stopping power value, calculate the remaining range of the ^{214}Po-α-particles after they cover the appointed distance. Remember to take the absorption layer thickness of the setup into account. From tables of the energies corresponding to these ranges, determine the stopping power of air. Use this value to convert the distance calibration curve into an energy calibration curve. Estimate the uncertainties. Compare the slope of the curve with the calibration constants you determined previously.

5. Determine the average range of the ^{214}Po-α-particles according to fig. 11. To do this, integrate the areas below the peaks of the ^{214}Po-α-particles for each recorded distance. Estimate the uncertainties and compare the result to values obtained from literature.

7.1.2 Ionisation chamber

1. Plot the measured currents as a function of the corresponding distances and discuss the curves. Why are there plateaus?

2. Use the plot to determine distance at which no ^{214}Po-α-particles reach the detector anymore. Use this distance to estimate the air equivalent of the thickness of the **additional** absorbing material between source and detector.

3. Use fig. 11 to determine the average range of the ^{214}Po-α-particles. Again, estimate the uncertainties.

4. Compare your results to those obtained with the semiconductor detector. Are your results compatible?

7.2 Scintillation counter measurements

1. Discuss the energy spectra of ^{137}Cs for each of the scintillation counters. Which peaks do you expect?

2. Determine the detection probability ε of the plastic scintillator relative to the NaI(Tl) counter, e.g. by using the count rate. Determine the light yield of the plastic scintillator in relation to the NaI(tl) counter, e.g. by using the position of the photo peak.

3. Determine the absorption coefficient μ and the mass absorption coefficient μ' the ^{137}Cs-γ-radiation in lead.

4. Determine the mass absorption coefficient μ' for measured β-radiation in aluminum.
   To do this, plot the absorption curve of ^{90}Sr-β-radiation including all necessary corrections. Use this plot to determine the maximal energy of the β-spectrum. Why do the measured values not follow an exponential distribution? When fitting the spectrum, it may be a good idea to provide starting values.

5. For the highest energetic β-particles from ^{90}Sr-decays, determine the range in aluminum. Compare the result with your measurement.

7.3 Radiation protection measurements

Report all measured dose rates. Are the used safes sufficient to shield the sources they contain? Are students sufficiently protected when they perform experiments? Were contaminations found?

Appendix

A Properties of radioactive sources used in the lab course

- ^{226}Ra: Open source, covered in a way that prevents touching. In the casing, there are three holes forming an equilateral triangle (side length $3{,}50 \pm 0{,}05\,\mathrm{mm}$). Each of the holes has a diameter of $2{,}1 \pm 0{,}05\,\mathrm{mm}$. The source is situated $4{,}5\,\mathrm{mm}$ below the holes, it is covered by a foil of $1{,}8 \pm 0{,}2\,\mu\mathrm{m}$ of chrome ($\rho = 7{,}1\,\mathrm{g/cm^3}$). Decay chain:

$$^{226}\mathrm{Ra} \xrightarrow{\alpha\,(4{,}78\,\mathrm{MeV})} {}^{222}\mathrm{Rn} \xrightarrow{\alpha\,(5{,}49\,\mathrm{MeV})} {}^{218}\mathrm{Po} \xrightarrow{\alpha\,(6{,}0\,\mathrm{MeV})} {}^{214}\mathrm{Pb} \xrightarrow{\beta^-\,(0{,}7\,\mathrm{MeV})} {}^{214}\mathrm{Bi} \xrightarrow{\beta^-\,(3{,}2\,\mathrm{MeV})}$$

$$^{214}\mathrm{Po} \xrightarrow{\alpha\,(7{,}69\,\mathrm{MeV})} {}^{210}\mathrm{Pb} \xrightarrow{\beta^-\,(0{,}02\,\mathrm{MeV})} {}^{210}\mathrm{Bi} \xrightarrow{\beta^-\,(1{,}16\,\mathrm{MeV})} {}^{210}\mathrm{Po} \xrightarrow{\alpha\,(5{,}3\,\mathrm{MeV})} {}^{206}\mathrm{Pb}$$

  ^{222}Rn is gaseous under normal conditions. The chrome foil prevents the gas to leave the casing.

- ^{90}Sr: Source fully encased in plexiglas pane, which in turn is encased in a steel sheet. Decay chain:

$$^{90}\mathrm{Sr} \xrightarrow{\beta^-\,(0{,}55\,\mathrm{MeV})} {}^{90}\mathrm{Y} \xrightarrow{\beta^-\,(2{,}27\,\mathrm{MeV})} {}^{90}\mathrm{Zr}$$

- ^{137}Cs: Source fully encased in plexiglas pane.

$$^{137}\mathrm{Cs} \xrightarrow{\beta^-\,(0{,}51\,\mathrm{MeV})} {}^{137}\mathrm{Ba}^{*} \xrightarrow{\gamma(0{,}66\,\mathrm{MeV})} {}^{137}\mathrm{Ba}$$

- ^{241}Am: Open source, covered in a way that prevents touching. Face side diameter of $1\,\mathrm{mm}$. The source is situated $1{,}5\,\mathrm{mm}$ under a gold ($\rho = 19{,}3\,\mathrm{g/cm^3}$) cover foil of thickness $3\,\mu\mathrm{m}$.

B Properties of the semiconductor detector

A Si-pin photodiode with an absorption depth of about $300\,\mu\mathrm{m}$ is used as detector. The radiation inlet window consists of $6\,\mu\mathrm{m}$ kapton and $0{,}5\,\mu\mathrm{m}$ aluminum. Power is supplied via a mains adaptor. Signal and supply lines use a shared cable. Possible output signals are either a spectroscopy signal (analog, used here) or a TTL signal with all pulses above the chosen threshold. The detector (including the complete spectroscopy amplification electroncis) is operated with a bias voltage of $\pm 5\,\mathrm{V}$ and $-80\,\mathrm{V}$.

Beside the known and accesible details of detector design, additional aspects may cause energy losses. Aging processes, the passivation layer and electronic contacts are possible sources.

C Properties of the collimator

The collimator consists of a brass pan head screw M6. Into the screw, a hole with a diameter of $2{,}50 \pm 0{,}05\,\mathrm{mm}$ is drilled. A plastic mount is used as an adapter for installation on the casing of the ^{226}Ra source.

D Properties of the aluminum absorber

Absorber	Area mass density in mg/cm^2	Thickness in mm
1-4	(defective)	
5	6,84	0,03
6	10,7	0,04
7	13,2	0,05
8	22,9	0,08
9	28,2	0,10
10	45,6	0,17
11	66,8	0,25
12	100	0,37
13	135	0,50

Absorber	Area mass density in mg/cm^2	Thickness in mm
14	174	0,64
15	224	0,83
16	274	1,01
17	332	1,23
18	375	1,39
19	423	1,57
20	507	1,88
21	617	2,29
22	754	2,79
23	933	3,46

E Description of the NIM modules

In nuclear and particle physics, there is an established standard for mechanical dimensions and electric signals: Nuclear Instrument Modules (NIM). In this standard, the spatial dimensions of each module consistent, so that all modules fit into the same mounts. Power supply plugs are also standardised. Power is supplied by the frame that supports the individual modules. The frame is called NIM crate.

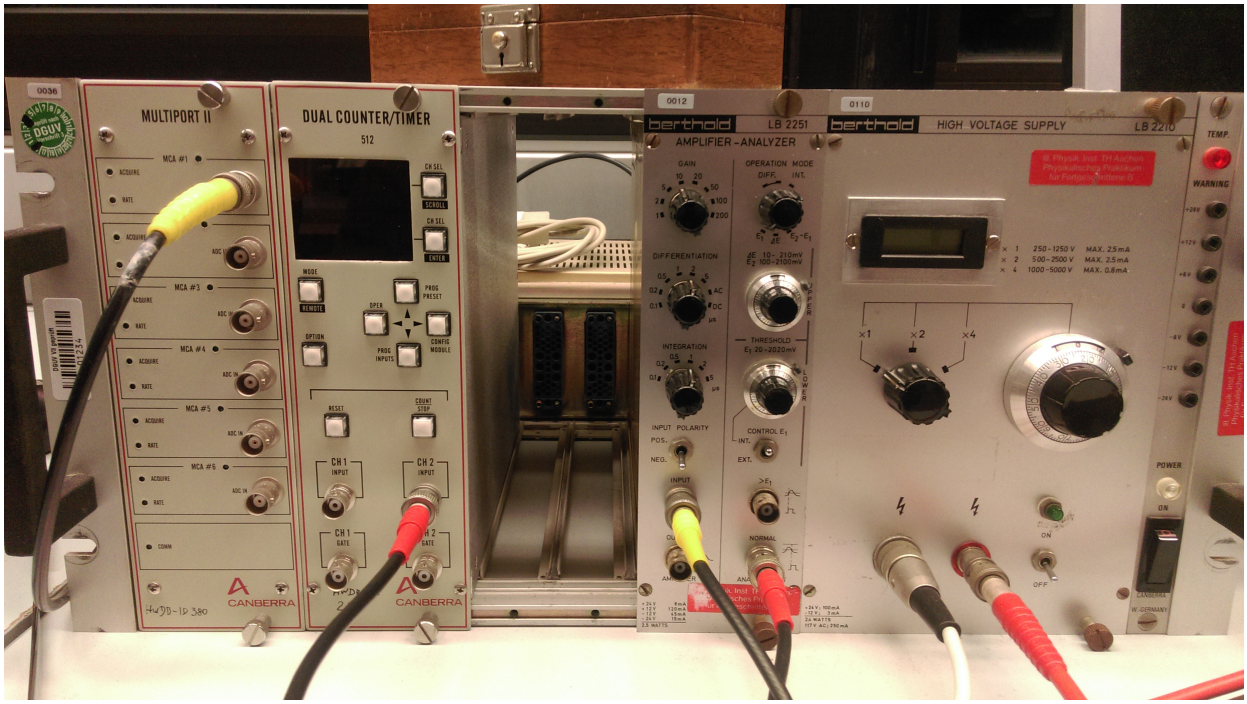

Figure 13: NIM crates used in T1.

The experiment TI uses different NIM modules for Al absorption measurement (see fig. 13): a Multiport, a Dual Counter and timer, an amplifier, pulse shaper and discriminator, and a power supply.

- **Multiport**: (fig. 13 - 1) The Multiport II module contains an analog-digital converter. Its digital output signal is proportional to the amplitude of the analog input pulse and therefore proportional to the energy deposited in the scintillator. Before conversion, the input signal must be amplified and its shape must be formed (see below). The output signal is processed by the multi-channel

analyzer (MCA), which transmits the data via USB to the PC. On the PC, the measured values may be viewed using Genie 2000. More details about the Multiport II module may be found at: `http://www.canberra.com/products/radiochemistry_lab/nim-multichannel-analyzer.asp`

- **Counter**: (fig. 13 - 2) This modules counts the number of measured pulses. In order for this to work, the signal of the scintillation counters needs to be converted into logic pulses (see *Amplifier and puls shaper* and *Discriminator*). Beware: The analog signal of the scintillation counter **must not** be used as input!
  Pulses are counted during a preset measurement time. The preset may be changed like this: Press 'Mode' and shortly after 'Prog/Preset'. The corresponding button should light up and the display should read 'Prog/Preset'. Using the 'Scroll' button, until the display reads 'Std/Timer A' and confirm with the 'Enter' button. The desired measurement time may then be set using the arrow buttons. To save the value, press 'Enter'. To leave the menu press 'Exit' and confirm with 'Enter'. A measurement is started using the 'Count/Stop' button. Before starting another measurement, reset the counter by pressing 'Reset' and 'Count/Stop'.

- **Amplifier and pulse shaping**: (fig. 13 - 3a) The signal of the scintillation counter are in the mV range and need to be amplified. To do this, multiple gain settings are available with the amplifier module. Ideally, the gain should be chosen so that the energy range of the MCA is fully used. When using the counter, the setup should be optimised to deliver high rates.
  To obtain appropriate pulse length and amplitude, differentiation and integration time may be varied. The differentiation time setting allows for separation of close-by pulses. The integration time should be chosen high enough for all ions to be collected but low enough for the counting rate to remain high. The pulse polarity may be toggled using the 'positiv/negativ' switch. The pulse shape should be checkes using the oscilloscope.

- **Discriminator**: (fig. 13 - 3b) The discriminator allows for the creation of logic signals for counter input and filtering of the noisy PM signal. There are multiple modes that either use a threshold trigger on the rising flank or an interval trigger on the falling flank of the pulse. The value of the threshold may be varied. The output is a digital pulse.

- **Voltage supply**: (fig. 13 - 4) The photo-multipliers (PMT) are operated with a **maximal** voltage of 1200 V. The voltage may be set using a rotary dial and one of three multiplication factors. The voltage shown in the display is the one that is actually applied. When turning the device on or off, be **gentle**: avoid sharp jumps, slowly turn down/up the voltage before/after turning off/on.

Another NIM crate is also used for the gamma spectrum measurement (see fig. 14):

- **HV supply**: (fig. 14 - 1) In this setup the PMT with a lower HV : the working point is 600 V. Only the bottom's button is to be used. Please notice that the display is directly in kV. This module is connected in the back to the detector.

- **Amplifier and pulse shaping**: (fig. 14 - 2) The coarse gain as well as the fine gain can be adjusted. The polarity and the time window can be modified as well.

- **Multiport**: (fig. 14 - 3) Identical as described above.

F Genie 2000: Gamma measurements and analysis

The Genie 2000 software is used in the measurement of decay spectra. It is started by clicking on the "Gammamessung & -analyse" icon on the desktop.
When starting the software, the detector may not be selected already, which means you cannot start a measurement using the "Start" button. In this case, do: Datei → Datenquelle öffnen → Quelle: Detektor → MP2_MCA1 öffnen → measure.

Measurement settings may also be changed in the program. First of all, turn on the high voltage : in "MCA" (or "VKA")then in "Adjust", choose HVPS and then click "on". In "VKA" → "Messung-Vorwahl"

Figure 14: NIM crates used in T1.

you can change the number of channels and the measurement time. Remember that the livetime value already takes into account deadtime, while the realtime value tells you how long the measurement has been running.

Under "VKA" → "Einstellen" there are some more useful settings. Using LLD (Lower Level Discriminator, in % of the full measurement scale) and ULD (Upper Level Discriminator), possible signal noise can be minimised. When using these settings, it is important to make sure that no part of the signal is lost. Give all your settings in the report.
Measurements may be saved as "TKA" file, which is an ASCII file containing columns of data. The first two columns are live and real time. The following columns are the channel entries.

G Bethe-Bloch formula

The Bethe-Bloch formula may be used to calculate the energy loss of α-particles in air:

$$-\frac{dE}{dx} = \kappa\,\rho\,\frac{Z}{A}\,\frac{z^2}{\beta^2}\left[\ln\left(\frac{2m_\mathrm{e}c^2\gamma^2\beta^2}{I}\right)\right] \tag{20}$$

Where

- $\kappa = 2\pi\,N_0\,{r_\mathrm{e}}^2\,m_\mathrm{e}\,c^2 = 0{,}154\,\mathrm{MeV\,cm^2/g}$,
- $\rho = 1{,}225\cdot 10^{-3}\,\mathrm{g/cm^3}$ mass density of air near the ground,
- Z Charge number of air (mainly nitrogen),
- $m_\mathrm{e}c^2 = 0{,}511\,\mathrm{MeV}$ mass of the electron,
- $I \approx 15\,\mathrm{eV}$ mean ionisation potential of air,
- A atomic weight of air,
- z charge number of the traversing particle,

- $\beta = \sqrt{E_\alpha / \frac{1}{2} m_\alpha c^2}$ velocity of the traversing particle in units of the speed of light in vacuum ($E_\alpha$is the energy and m_α the mass of α-particles) and
- $\gamma = 1/\sqrt{1-\beta^2}$ is the Lorentz factor.

Note that this formula is only approximate and should only be used for qualitative arguments. Especially for small energies, effects from atomic physics cause large corrections. Therefore, it is a good idea to use energy loss values for α-particles from appropriate tables in literature. E.g. on the website of the *National Institute of Standards and Technology* [10].